Editors' Suggestion

Fracton Self-Statistics

Hao Song,[1,2] Nathanan Tantivasadakarn,[3,4,5] Wilbur Shirley,[6,4,7] and Michael Hermele[8]
[1]CAS Key Laboratory of Theoretical Physics, Institute of Theoretical Physics, Chinese Academy of Sciences, Beijing 100190, China
[2]Department of Physics and Astronomy, McMaster University, Hamilton, Ontario L8S 4M1, Canada
[3]Walter Burke Institute for Theoretical Physics, California Institute of Technology, Pasadena, California 91125, USA
[4]Department of Physics, California Institute of Technology, Pasadena, California 91125, USA
[5]Department of Physics, Harvard University, Cambridge, Massachusetts 02138, USA
[6]School of Natural Sciences, Institute for Advanced Study, Princeton, New Jersey 08540, USA
[7]Institute for Quantum Information and Matter, California Institute of Technology, Pasadena, California 91125, USA
[8]Department of Physics and Center for Theory of Quantum Matter, University of Colorado, Boulder, Colorado 80309, USA

(Received 10 July 2023; accepted 14 December 2023; published 5 January 2024)

Fracton order describes novel quantum phases of matter that host quasiparticles with restricted mobility and, thus, lies beyond the existing paradigm of topological order. In particular, excitations that cannot move without creating multiple excitations are called fractons. Here, we address a fundamental open question—can the notion of self-exchange statistics be naturally defined for fractons, given their complete immobility as isolated excitations? Surprisingly, we demonstrate how fractons can be exchanged and show that their self-statistics is a key part of the characterization of fracton orders. We derive general constraints satisfied by the fracton self-statistics in a large class of Abelian fracton orders. Finally, we show the existence of nontrivial fracton self-statistics in some twisted variants of the checkerboard model and Haah's code, establishing that these models are in distinct quantum phases as compared to their untwisted cousins.

DOI: 10.1103/PhysRevLett.132.016604

Introduction.—Particle statistics is a fundamental aspect of quantum mechanics. While elementary particles that compose our Universe must be either bosons or fermions due to the topological triviality of double exchanges in 3D space, emergent quasiparticles in 2D quantum many-body systems can exhibit anyonic statistics [1,2], which are crucial for characterizing conventional topological order. Recently, the theoretical discovery of fracton order in 3D [3–9] has revealed a new situation where quasiparticles lack their usual freedom to move in space, calling for a reexamination of the notion of statistics [10–12].

Fracton systems have emerged as an active frontier of quantum physics [13,14], attracting great interest from condensed matter, quantum information, and quantum field theory viewpoints. Fracton order is defined by the emergence of quasiparticles with restricted mobility, including *fractons*, which cannot move without splitting into more than one excitation. Single isolated fractons are, thus, immobile. Fracton models can also host excitations which are mobile only within planes or lines. Statistical processes involving or interpretable in terms of partially mobile excitations have been studied [10–12,15–23]. Moreover, fractons can be non-Abelian in the sense of carrying protected topological degeneracy [11,16,24–35]. Nevertheless, a fundamental question remains open: Does a notion of self-exchange statistics make sense for fractons, given their complete immobility as isolated excitations?

In this Letter, we provide a resolution to this puzzle. By allowing the fracton quasiparticle to split into multiple coordinated pieces, it is possible to prepare two well-separated realizations of the same fracton superselection sector. Such a pair of excitation patterns can be physically exchanged, giving rise to a fracton self-statistics. Our findings apply to both fracton phases of foliated [36,37] and fractal [5,6] nature. Furthermore, we point out instances where the self-statistics of fractons is, in fact, the only known statistical invariant that distinguishes between two fracton phases. We provide explicit examples by distinguishing twisted checkerboard models [11] and a twisted Haah's code [38] from their untwisted counterparts. Thus, we show that fracton self-statistics is a fundamental invariant needed to characterize fracton phases of matter.

Foliated fractons.—To illustrate the principle, we start with the simplest relevant setting, in which all fractons a are Abelian [39] and satisfy the fusion constraint

$$a \times \overline{{}^{\mathbf{t}_\mu} a} \times {}^{\mathbf{t}_\mu+\mathbf{t}_\nu} a \times \overline{{}^{\mathbf{t}_\nu} a} = 1 \tag{1}$$

for all $\mu, \nu \in \{x, y, z\}$ such that $\mu \neq \nu$, where $\mathbf{t}_{\mu(\nu)}$ is the elementary lattice vector in the $\mu(\nu)$ direction, ${}^{\mathbf{t}}a$ denotes the analog of a at a $\mathbf{t}$-shifted position, and $\overline{{}^{\mathbf{t}}a}$ is the antiparticle of ${}^{\mathbf{t}}a$. This constraint guarantees the existence of rectangular [40] membrane operators of arbitrary size that generate quadrupolar configurations of a given species a at its corners. Fractons satisfying the fusion constraint will be referred to as (Abelian) *foliated*.

A large body of models hosting foliated fractons are known in the literature, including the X-cube,

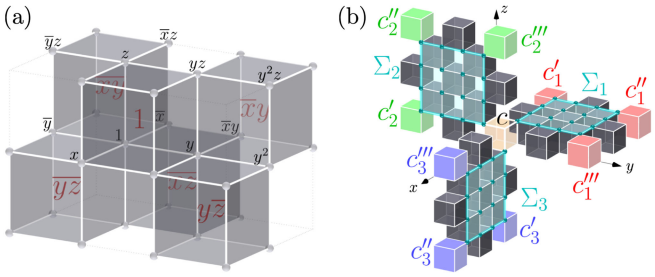

FIG. 1. (a) 3D checkerboard lattice with vertices and gray cubes labeled by monomials $x^j y^k z^l$, where $\bar{x} \equiv x^{-1}$, etc. (b) In the checkerboard model, excitation $A_c = -1$ (or $B_c = -1$) has *fractional mobility* $\{c\} \to \{c_i', c_i'', c_i'''\}$, realizable by operator $M_i = \prod_{v \in \Sigma_i} Z_v$ (respectively, $M_i = \prod_{v \in \Sigma_i} X_v$) supported on rectangular membrane Σ_i, for $i = 1, 2, 3$.

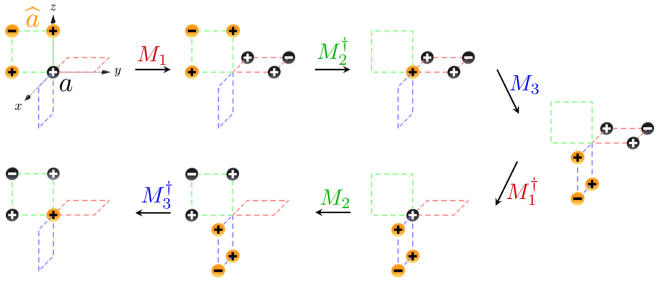

FIG. 2. The $[xyz]$ windmill process. The starting state has an excitation a at the center of the "windmill" along with three other excitations collectively called $\hat{a}$ in the same superselection sector as a following Eq. (1). The process involves three membrane operators M_1, M_2, and M_3 and their inverses, successively moving the four excitations from the corners of the yz square, to the corners of the xy square, to the corners of the zx square, and finally back to the original configuration. The process is designed such that the phase arbitrariness in the choice of M_i is precisely canceled by the action of $M_i^\dagger$. Therefore, the universal statistical phase is well defined by $\theta_a^{[xyz]} = M_3^\dagger M_2 M_1^\dagger M_3 M_2^\dagger M_1$.

checkerboard, and their many variants [8,11,17,41–43]. Let us refer to the checkerboard model as a concrete example, for its twisted variants will clearly demonstrate the usage of fracton self-statistics.

The *checkerboard model* [8] is defined on a 3D checkerboard lattice [Fig. 1(a)] with one qubit per vertex v. Its Hamiltonian

$$H_{\mathrm{cb}} = -\sum_c (A_c + B_c) \tag{2}$$

is a summation over gray cubes c in Fig. 1(a), where

$$A_c := \prod_{v \in c} X_v, \qquad B_c := \prod_{v \in c} Z_v \tag{3}$$

are products of Pauli X or Z operators at the eight vertices of c. This is an exactly solvable gapped model with spectrum labeled by simultaneous eigenvalues $\{A_c, B_c = \pm 1\}$.

An isolated excitation $A_c = -1$ exemplifies a foliated fracton. It can be "moved" at the expense of fractionalizing into more than one excitation, e.g., $\eta = \{c\} \to \eta_i = \{c_i', c_i'', c_i'''\}$ by a rectangular membrane operator; see Fig. 1(b). Therefore, the excitation patterns η_1 (red), η_2 (green), η_3 (blue), and η (orange) are all realizations of the same fracton superselection sector.

Self-statistics of foliated fractons.—Generically, a foliated fracton a is characterized by a set of four self-statistical phases $\theta_a^{[xyz]}$, $\theta_a^{[x\bar{y}\bar{z}]}$, $\theta_a^{[\bar{x}y\bar{z}]}$, and $\theta_a^{[\bar{x}\bar{y}z]}$, each corresponding to a "windmill" self-exchange process.

The process corresponding to $\theta_a^{[xyz]}$ is depicted in Fig. 2. It begins with an excited state with a at the center of the windmill, in addition to a triplet of excitations denoted $\hat{a}$ that belongs to the same superselection sector as a. The process proceeds with a sequence of six membrane operators [Fig. 3(a)] whose total action exchanges a with $\hat{a}$, returning to the starting state in such a way that all arbitrary phases cancel. It can be regarded as a fractonic generalization of the T-shaped anyon exchange process [44].

The processes for $\theta_a^{[x\bar{y}\bar{z}]}$, $\theta_a^{[\bar{x}y\bar{z}]}$, and $\theta_a^{[\bar{x}\bar{y}z]}$ are defined analogously but along windmills related to $[xyz]$ by a 180° rotation about the x, y, and z axes, respectively. For instance, the $[x\bar{y}\bar{z}]$ process involves the membrane operators located as in Fig. 3(b). The notation $[\mu_1\mu_2\mu_3]$ of three directions μ_i refers to a windmill made of three blades $K_i = \mathrm{cone}(-\boldsymbol{\mu}_i, \boldsymbol{\mu}_{i+1}) \equiv \{-\alpha\boldsymbol{\mu}_i + \beta\boldsymbol{\mu}_{i+1} | \alpha, \beta \geq 0\}$ for $i = 1, 2, 3$, where $\mu_4 \equiv \mu_1$. Each overlined direction indicates its opposite (e.g., $\bar{\mathbf{x}} = -\mathbf{x}$).

Although more windmill processes can be considered, they yield *no* new self-statistical phases beyond the four already defined. Any two inversion-related windmills [e.g., $[xyz]$ and $[\bar{x}\bar{y}\bar{z}]$ in Figs. 3(a) and 3(c)] specify the same self-statistics. The reason is demonstrated in Fig. 3(d): Membrane operators for $[xyz]$ and $[\bar{x}\bar{y}\bar{z}]$ can be related by a deformation [45]. Consequently, despite eight possible windmill choices (see Supplemental Material [46]), only four self-statistics need to be specified for foliated fractons.

One might expect that $\theta_a^{[xyz]}$, $\theta_a^{[x\bar{y}\bar{z}]}$, $\theta_a^{[\bar{x}y\bar{z}]}$, and $\theta_a^{[\bar{x}\bar{y}z]}$ are independent. To the contrary, they are subject to a constraint

$$\theta_a^{[xyz]} \theta_a^{[x\bar{y}\bar{z}]} \theta_a^{[\bar{x}y\bar{z}]} \theta_a^{[\bar{x}\bar{y}z]} = 1, \tag{4}$$

leaving only three of them independent, in general.

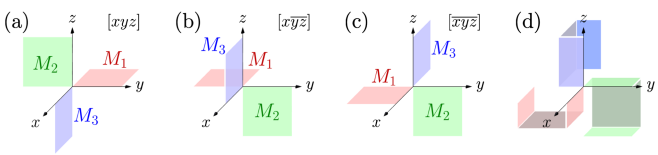

FIG. 3. Membrane operators comprising the (a) $[xyz]$, (b) $[x\bar{y}\bar{z}]$, and (c) $[\bar{x}\bar{y}z]$ windmill processes. (d) The membrane operators for the $[\bar{x}\bar{y}z]$ process are smoothly deformed such that, near the origin, they coincide with those of the $[xyz]$ process. This proves $\theta_a^{[\bar{x}\bar{y}z]} \equiv \theta_a^{[xyz]}$.

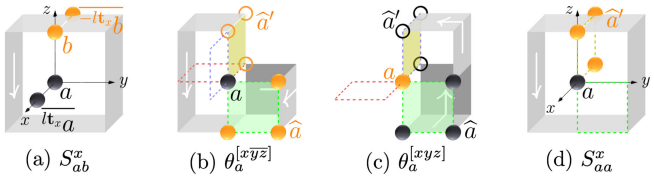

FIG. 4. Graphic proof of $\theta_a^{[x\overline{yz}]}\theta_a^{[xyz]} = S^x_{aa}$. The white arrows denote the direction of braiding and exchange processes. (a) Definition of S^x_{ab}. (b) The $[x\overline{yz}]$ process (dotted windmill) is deformable into one realized in three steps $a \to \hat{a}'$, $\hat{a} \to a$, and $\hat{a}' \to \hat{a}$ using operators supported on the olive, green, and gray areas. The intermediate state $\hat{a}'$ consists of excitations at the three circles. (c) A process which is equivalent to the $[\overline{xyz}]$ process and, hence, produces statistics $\theta_a^{[\overline{xyz}]} \equiv \theta_a^{[xyz]}$. (d) A process that braids part of $\hat{a}'$, along on the gray ribbon, around a. The statistical phase due to the presence of a is S^x_{aa}.

This constraint is most naturally derived by utilizing a quantity S^μ_{ab} for $\mu = x, y, z$, defined as the mutual braiding statistics between dipoles $a \times \overline{\mathbf{t}_\mu a}$ and $b \times \overline{-l\mathbf{t}_\mu b}$ in the large l limit. The dipoles are planons (i.e., quasiparticles mobile in two directions). The braiding direction is fixed by μ via the right-hand rule. See Fig. 4(a).

A proof of Eq. (4) is as follows. If a is exchanged twice with $\hat{a}$, both sets of excitations return to their original position. The total process is smoothly deformable into one where a is stationary while $\hat{a}$ braids around a. For instance, we can deform the $[x\overline{yz}]$ windmill process into one along the cyclic "path" in Fig. 4(b). Similarly, the $[\overline{xyz}]$ process (which produces statistics $\theta_a^{[\overline{xyz}]} \equiv \theta_a^{[xyz]}$) is deformable into the one depicted in Fig. 4(c). If the two deformed exchanges are started and ended with the intermediate state containing excitations a and $\hat{a}'$, their composite gives the process in Fig. 4(d), implying

$$\theta_a^{[xyz]}\theta_a^{[x\overline{yz}]} = S^x_{aa}. \tag{5}$$

Armed with this relation, we can now prove Eq. (4) by a 180° rotation of Eq. (5) about the y axis to obtain $\theta_a^{[\bar{x}yz]}\theta_a^{[\overline{\bar{x}yz}]} = (S^x_{aa})^*$ and multiplying it with Eq. (5).

The mutual statistics also appear in the following formula for the self-statistics of a fusion product of two fractons and analogous formulas due to cubic symmetry:

$$\theta^{[xyz]}_{a\times b} = \theta^{[xyz]}_a \theta^{[xyz]}_b S^x_{ab} S^y_{ab} S^z_{ab}. \tag{6}$$

See Supplemental Material [46] for a proof. This relation implies

$$S^x_{ab} S^y_{ab} S^z_{ab} = S^x_{ba} S^y_{ba} S^z_{ba}. \tag{7}$$

It is interesting to note that Eqs. (5) and (6) generalize the constraints $\theta_a^2 = S_{aa}$ and $\theta_{a\times b} = \theta_a \theta_b S_{ab}$ of 2D Abelian topological orders, where θ_a is the topological spin and S the topological S matrix. For an Abelian planon a satisfying the foliation condition Eq. (1), analogous windmill processes are reducible into 2D braidings, and the above discussions reduce to these familiar 2D equations.

Now assume a foliated fracton satisfies $a^N = 1$. We show its self-statistics being constrained to *discrete* values for use in distinguishing fracton orders. Note $S^x_{aa} S^y_{aa} S^z_{aa} = (\theta_a^{[xyz]})^2$ by virtue of Eqs. (4) and (5). Thus, since $(S^\mu_{aa})^N = S^\mu_{a^N a} = 1$, we have $(\theta_a^{[xyz]})^{2N} = 1$. Moreover, applying Eq. (6) recursively gives $(\theta_a^{[xyz]})^{N^2} = \theta_{a^N}^{[xyz]} = 1$. Together, these imply the self-statistics of a being multiples of $e^{2\pi i/(N \gcd(N,2))}$ in analogy to anyons in 2D.

Semionic fractons in twisted checkerboard models.—A major application of fracton self-statistics is to distinguish the quantum phase of the checkerboard model H_{cb} from its twisted variants introduced in Ref. [11]. To illustrate, we consider seven twisted models, denoted H^x_{cb}, H^y_{cb}, H^z_{cb}, H^{xy}_{cb}, H^{yz}_{cb}, H^{zx}_{cb}, and H^{xyz}_{cb} below. Together with H_{cb}, we will show that the eight models fall into two quantum phases, distinguishable by the presence or absence of semionic fracton self-statistics. Explicit construction of paths connecting models with identical fracton self-statistics is given in Supplemental Material [46].

First, in H_{cb} [Eq. (2)], all excitations (including fractons) exhibit either bosonic $(+1)$ or fermionic (-1) statistics. This is because all statistical processes are realizable by tensor products of Pauli operators which commute or anticommute only with each other.

In contrast, H^x_{cb} represents a new phase allowing *semionic* $(\pm i)$ fracton self-statistics. Instead of using the formalism in Ref. [11], we specify this model using a non-Pauli stabilizer Hamiltonian

$$H^x_{\mathrm{cb}} = -\sum_c (A^x_c + B_c) \tag{8}$$

obtained by replacing A_c in the untwisted model Eq. (2) with a modified term A^x_c, to have a convenient description of excitations with $(A^x_c)^2 = 1$ and the full spectrum labeled by simultaneous eigenvalues $\{A^x_c, B_c = \pm 1\}$, where x refers to twisting being associated with x edges. Explicitly, we label vertices and cubes by monomials as in Fig. 1(a) and denote finite sets of vertices by polynomials with $\mathbb{Z}_2 = \{0, 1\}$ coefficients [55]. In this notation,

$$A^x_c \coloneqq A_c \phi_{(1+x)\bar{x}c} \phi_{(1+x)xc} \tag{9}$$

according to the construction described in Supplemental Material [46], where $\ell = (1+x)\bar{x}c$ and $\ell = (1+x)xc$ denote vertex pairs that are ends of x edges and

$$\phi_\ell \coloneqq (-1)^{n^-_{\ell\bar{y}} n^-_\ell + n^-_{\ell\bar{y}z} n^-_{\ell z} + n^-_\ell n^+_{\ell y} + n^-_{\ell z} n^+_{\ell yz} + n^+_{\ell y} n^-_{\ell y^2} + n^+_{\ell yz} n^-_{\ell y^2 z}} \cdot (-1)^{n^-_{\ell yz(1+y)} n^-_{\ell y(1+y)(1+z)}} \cdot i^{-n^-_{\ell(1+\bar{y})(1+z)}} \tag{10}$$

is a Dijkgraaf-Witten twisting factor, with the shorthand

$$Z_\kappa := \prod_{v\in\kappa} Z_v, \qquad n_\kappa^{\pm} := \frac{1}{2}(1 \pm Z_\kappa), \tag{11}$$

for κ any finite set of vertices.

In H^x_{cb}, one example of semionic fracton is a $B_c = -1$ excitation (denoted m_x below), which has

$$\theta^{[xyz]}_{m_x} = \theta^{[x\overline{yz}]}_{m_x} = i \quad \text{and} \quad \theta^{[\overline{xy}z]}_{m_x} = \theta^{[\bar{x}y\bar{z}]}_{m_x} = -i. \tag{12}$$

Two derivations of the statistics are given in Supplemental Material [46]. In one, we construct a modified X operator that explicitly generates the statistical processes for B excitations. The modification of X is required to ensure no A^x_c terms flipped and results in the above semionic self-statistics.

We emphasize that, in H^x_{cb}, exotic self-statistics ($\theta \neq \pm 1$) are exclusive to fractons. Reference [11] reported that nonfractonic excitations in H^x_{cb} exhibit only bosonic or fermionic statistics. This implies that H^x_{cb} cannot be a tensor product of H_{cb} and 2D anyon models containing semions. Therefore, the fact that only fracton self-statistics can distinguish the two models highlights the novelty of H^x_{cb} as a distinct phase of matter. We refer to the phase of H^x_{cb} as a *semionic fracton order*, as characterized by the presence of semionic statistics for only the fracton excitations.

The remaining six models are constructed similarly to H^x_{cb}. In H^x_{cb}, the twisting factor $\phi_{(1+x)\bar{x}c}\phi_{(1+x)xc}$ in Eq. (9) is linked to x edges. Its analog associated with y edges (z edges) specifies H^y_{cb} (H^z_{cb}). Moreover, twisting can be applied to more than one direction simultaneously; for example, H^{xy}_{cb} has twisting made along both x edges and y edges.

Remarkably, despite the six models having different ground states, we discover that (i) H^y_{cb}, H^z_{cb}, and H^{xyz}_{cb} represent the same semionic fracton phase as H^x_{cb}, while (ii) H^{xy}_{cb}, H^{yz}_{cb}, and H^{zx}_{cb} fall within the phase of H_{cb}. Let us first demonstrate how fracton self-statistics are matched between H^{xy}_{cb} and H_{cb}. In H^{xy}_{cb}, excitation $B_c = -1$ (denoted m_{xy}) is a fracton with

$$\theta^{[xyz]}_{m_{xy}} = i\cdot i = -1, \qquad \theta^{[\overline{xy}z]}_{m_{xy}} = (-i)^2 = -1,$$
$$\theta^{[x\overline{yz}]}_{m_{xy}} = i\cdot(-i) = 1, \qquad \theta^{[\bar{x}y\bar{z}]}_{m_{xy}} = (-i)\cdot i = 1, \tag{13}$$

where two twistings cause a cancellation in semionic character. Furthermore, combining m_{xy} with an A excitation at relative position $\bar{x}y$, denoted ${}^{\bar{x}y}e$, yields a fracton ${}^{\bar{x}y}e \times m_{xy}$ with purely bosonic self-statistics, which can be seen via Eq. (6) and its analogs.

Based on this observation, we indeed find an exact local unitary transformation relating the ground states of H^{xy}_{cb} and H_{cb}, rigorously confirming they represent the same phase

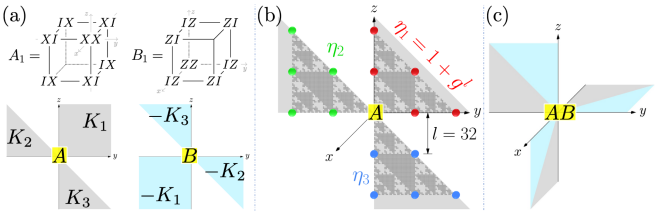

FIG. 5. Fracton's mobility in the Haah's code. (a) Top: definition of A_1 and B_1. They are products of eight Paulis. Identity operators I are omitted when possible. Bottom: mobility cones (on the yz plane) for A and B excitations. (b) Fractional moves $1 \to \eta_i$ of an A excitation are realized by operators of fractal support. Gray square dots represent operator $(0, 0, y + z, 1)$ and its translations. (c) A windmill for a composite of type-A and type-B fractons.

(see Supplemental Material [46]). Other phase identifications in the classification can be proven analogously.

Self-statistics of fractal fractons.—The notion of self-statistics extends to nonfoliated fractons [56]. We demonstrate this with Haah's code [5]

$$H_{\mathrm{Haah}} = -\sum_{\lambda\in\Lambda}(A_\lambda + B_\lambda), \tag{14}$$

an exactly solvable model defined on a cubic lattice with two qubits per vertex. Here, $\Lambda = \{x^i y^j z^k\}$ represents lattice vectors $(i, j, k) \in \mathbb{Z}^3$ in monomial form. The $A(B)$ terms are translations of the representative $A_1(B_1)$ at the origin given in Fig. 5(a). Each $A_\lambda(B_\lambda)$ is a product of eight Pauli X's (Z's). With collections of translationally related objects represented as sums of Λ's elements, we can describe A_λ and B_λ using Laurent polynomials with $\mathbb{Z}_2 = \{0, 1\}$ coefficients [55]:

$$A_\lambda = \lambda\cdot(\bar{f}_1, \bar{f}_2, 0, 0), \qquad B_\lambda = \lambda\cdot(0, 0, f_2, f_1), \tag{15}$$

$$f_1 = 1 + x + y + z, \qquad f_2 = 1 + xy + yz + zx, \tag{16}$$

$$\bar{f}_1 = 1 + \bar{x} + \bar{y} + \bar{z}, \qquad \bar{f}_2 = 1 + \overline{xy} + \overline{yz} + \overline{zx}, \tag{17}$$

where the first (last) two components of A_λ and B_λ locate Pauli X's (Z's) for the two qubit species. The bar denotes spatial inversion: $x \to \bar{x} \equiv x^{-1}$, etc.

Excitations can also be described by polynomials. Applying a Pauli Z to the first (or second) qubit at the origin excites A terms in the pattern f_1 (respectively, f_2). Interestingly, one may flip A terms purely in the yz plane [6] by noting

$$(y + z)f_1 + f_2 = 1 + y + y^2 + z + yz + z^2 =: g. \tag{18}$$

Consider planar fractional moves for visual clarity. The yz-planar ones are generated by g, allowing A excitations to travel arbitrarily long distances toward each of the *conic*

directions K_1, K_2, and K_3 in Fig. 5(a). Explicitly, for $l = 2^n$, one has $1 + g^l = y^l + y^{2l} + z^l + z^l y^l + z^{2l}$ due to the $\mathbb{Z}_2$ setting of the model. Accordingly, $1 \to 1 + g^l$ provides an instance of pushing an A-term excitation by at least l distance toward K_1. It is realizable by fractal-shaped operator $g^{l-1}(0, 0, y + z, 1)$, reflecting the excitation being a fracton of fractal nature. See Fig. 5(b). We call each K_i a *mobility cone* for A excitations, as defined in Supplemental Material [46]. The description of B excitations are analogous but with spatial directions inverted.

Based on mobility cones, we categorize fractons of H_{Haah} into three types—A, B, and mixed—and define their windmill self-statistical processes. Type A (type B) are fractons with the mobility cones K_i (respectively, $-K_i$) for $i = 1, 2, 3$ shown in Fig. 5(a). The mixed are bound states of type A and type B; they cannot be moved along any individual cone among K_i's or $-K_i$'s. Self-statistics is definable using the "windmill" made of mobility cones. See Figs. 5(a) and 5(c). In H_{Haah}, nonmixed (i.e., type-A or type-B) fractons exhibit purely bosonic self-statistics, since only one type of Pauli is involved.

Fermionic type-A fractons in a twisted Haah's code.—To further illustrate the usage of fracton self-statistics, consider a gauge-theoretic variant of Haah's code defined by applying H_{Haah} to a Hilbert space that binds a *fermionic* mode ψ_λ to A_λ via Gauss's law $-i\gamma_\lambda\tilde{\gamma}_\lambda A_\lambda = 1$, where $\gamma_\lambda := \psi_\lambda + \psi_\lambda^\dagger$ and $\tilde{\gamma}_\lambda := (1/i)(\psi_\lambda - \psi_\lambda^\dagger)$ are Majorana operators. As detailed in Supplemental Material [46], the gauge theory emerges from a spin model H^F_{Haah}, namely, the twisted Haah's code proposed in Ref. [38].

Fracton self-statistics enables us to settle the unresolved question of whether H^F_{Haah} represents a distinct fracton order from the original Haah's code H_{Haah}. The expectation that A excitation becomes fermionic is now definable and provable via windmill processes. The operator creating A excitations is modified to $Z_\sigma c_\sigma$ due to gauge invariance, where Z_σ denotes Pauli Z on qubit σ while c_σ denotes a product of γ_λ's that are associated with the Z_σ-flipped A terms. Still, one may wonder whether it is possible to compensate the statistics change by attaching B excitations to A. Indeed, this is the case for the 2D toric code and the checkerboard model, which we have shown above. However, it is not allowed here, because attaching type-B fractons alters the mobility of A. Thus, the presence of fermionic type-A fractons distinguishes H^F_{Haah} from H_{Haah}. See also Supplemental Material [46] for the discreteness of this self-statistics, which confirms the phase distinction.

Conclusions.—We have shown that it is possible to exchange two realizations of a fracton superselection sector via its fractional mobility. The notion of self-statistics for fractons can, thus, be introduced, which is essential in characterizing fracton orders. As applications, we studied a family of twisted checkerboard models and a twisted Haah's code, from which we revealed a novel phase of foliated nature—what we call a semionic fracton order—and a new fractal-type order characterized by emergent fermionic fractons. Our work marks a crucial step toward a full "algebraic theory of fractons" yet to be developed.

We thank Sheng-Jie Huang, Juven Wang, and especially Ashvin Vishwanath for helpful discussions. The authors are grateful to the Banff International Research Station, where this work began in 2020 at the workshop "Fractons and Beyond." H. S. also acknowledges discussions with Sung-Sik Lee. H. S. has been supported by the Natural Sciences and Engineering Research Council of Canada and the National Natural Science Foundation of China (Grant No. 12047503). N. T. is supported by the Walter Burke Institute for Theoretical Physics at Caltech. The work of M. H. is supported by the U.S. Department of Energy, Office of Science, Basic Energy Sciences (BES) under Grant No. DE-SC0014415. W. S. is supported by the Simons Collaboration on Ultra-Quantum Matter (UQM), which is a grant from the Simons Foundation (651444). The work of N. T., W. S., and M. H. also benefited from meetings of the UQM Simons Collaboration supported by Simons Foundation Grant No. 618615.

[1] D. Arovas, J. R. Schrieffer, and F. Wilczek, Phys. Rev. Lett. **53**, 722 (1984).
[2] A. Kitaev, Ann. Phys. (Amsterdam) **321**, 2 (2006).
[3] C. Chamon, Phys. Rev. Lett. **94**, 040402 (2005).
[4] S. Bravyi, B. Leemhuis, and B. M. Terhal, Ann. Phys. (Amsterdam) **326**, 839 (2011).
[5] J. Haah, Phys. Rev. A **83**, 042330 (2011).
[6] B. Yoshida, Phys. Rev. B **88**, 125122 (2013).
[7] S. Vijay, J. Haah, and L. Fu, Phys. Rev. B **92**, 235136 (2015).
[8] S. Vijay, J. Haah, and L. Fu, Phys. Rev. B **94**, 235157 (2016).
[9] M. Pretko, Phys. Rev. B **95**, 115139 (2017).
[10] H. Ma, E. Lake, X. Chen, and M. Hermele, Phys. Rev. B **95**, 245126 (2017).
[11] H. Song, A. Prem, S.-J. Huang, and M. A. Martin-Delgado, Phys. Rev. B **99**, 155118 (2019).
[12] S. Pai and M. Hermele, Phys. Rev. B **100**, 195136 (2019).
[13] R. M. Nandkishore and M. Hermele, Annu. Rev. Condens. Matter Phys. **10**, 295 (2019).
[14] M. Pretko, X. Chen, and Y. You, Int. J. Mod. Phys. A **35**, 2030003 (2020).
[15] K. Slagle and Y. B. Kim, Phys. Rev. B **96**, 195139 (2017).
[16] S. Vijay and L. Fu, arXiv:1706.07070.
[17] A. Prem, S.-J. Huang, H. Song, and M. Hermele, Phys. Rev. X **9**, 021010 (2019).
[18] W. Shirley, K. Slagle, and X. Chen, Ann. Phys. (Amsterdam) **410**, 167922 (2019).
[19] D. Bulmash and T. Iadecola, Phys. Rev. B **99**, 125132 (2019).
[20] Y. You, T. Devakul, F. Burnell, and S. Sondhi, Ann. Phys. (Amsterdam) **416**, 168140 (2020).
[21] W. Shirley, arXiv:2002.12026.

[22] N. Tantivasadakarn, W. Ji, and S. Vijay, Phys. Rev. B **103**, 245136 (2021).
[23] W. Shirley, X. Liu, and A. Dua, Phys. Rev. B **107**, 035136 (2023).
[24] D. Bulmash and M. Barkeshli, Phys. Rev. B **100**, 155146 (2019).
[25] A. Prem and D. J. Williamson, SciPost Phys. **7**, 68 (2019).
[26] J. Wang and K. Xu, Ann. Phys. (Amsterdam) **424**, 168370 (2019).
[27] J. Wang, K. Xu, and S.-T. Yau, Phys. Rev. Res. **3**, 013185 (2021).
[28] J. Wang and S.-T. Yau, Phys. Rev. Res. **2**, 043219 (2020).
[29] D. Aasen, D. Bulmash, A. Prem, K. Slagle, and D. J. Williamson, Phys. Rev. Res. **2**, 043165 (2020).
[30] X.-G. Wen, Phys. Rev. Res. **2**, 033300 (2020).
[31] J. Wang, Phys. Rev. Res. **4**, 023258 (2022).
[32] D. J. Williamson and M. Cheng, Phys. Rev. B **107**, 035103 (2023).
[33] D. T. Stephen, J. Garre-Rubio, A. Dua, and D. J. Williamson, Phys. Rev. Res. **2**, 033331 (2020).
[34] N. Tantivasadakarn, W. Ji, and S. Vijay, Phys. Rev. B **104**, 115117 (2021).
[35] Y.-T. Tu and P.-Y. Chang, Phys. Rev. Res. **3**, 043084 (2021).
[36] W. Shirley, K. Slagle, Z. Wang, and X. Chen, Phys. Rev. X **8**, 031051 (2018).
[37] Z. Wang, X. Ma, D. T. Stephen, M. Hermele, and X. Chen, Phys. Rev. B **108**, 035148 (2023).
[38] N. Tantivasadakarn, Phys. Rev. Res. **2**, 023353 (2020).
[39] Non-Abelian generalizations will be studied in the future.
[40] Generally, $\{x, y, z\}$ may be oblique axes, and, accordingly, membranes are parallelogrammatic. However, for convenience, we assume $\{x, y, z\}$ to be orthogonal in this Letter.
[41] Y. You, T. Devakul, F. Burnell, and S. Sondhi, Ann. Phys. (Amsterdam) **416**, 168140 (2020).
[42] W. Shirley, K. Slagle, and X. Chen, Phys. Rev. B **102**, 115103 (2020).
[43] T. Devakul, W. Shirley, and J. Wang, Phys. Rev. Res. **2**, 012059(R) (2020).
[44] See Fig. 10 in Ref. [2], for instance.
[45] They are matched $(M_1, M_2, M_3)_{\overline{[xyz]}} \sim (M_3, M_1, M_2)_{[xyz]}$ up to a permutation, leaving self-statistics unchanged.
[46] See Supplemental Material at http://link.aps.org/supplemental/10.1103/PhysRevLett.132.016604 for the counting of windmills for foliated fractons, a proof of Eq. (6), details of twisted checkerboard models, a mathematical treatment of mobility cones, details of the twisted Haah's code, and the discreteness of fracton self-statistics in both the phases of the Haah's code and its twisted variant, which contains additional Refs. [47–54].
[47] H. Yan, K. Slagle, and A. H. Nevidomskyy, arXiv:2211.15829.
[48] M. A. Levin and X.-G. Wen, Phys. Rev. B **71**, 045110 (2005).
[49] Y. Hu, Y. Wan, and Y.-S. Wu, Phys. Rev. B **87**, 125114 (2013).
[50] G. Dauphinais, L. Ortiz, S. Varona, and M. A. Martin-Delgado, New J. Phys. **21**, 053035 (2019).
[51] J. C. M. de la Fuente, N. Tarantino, and J. Eisert, Quantum **5**, 398 (2021).
[52] T. D. Ellison, Y.-A. Chen, A. Dua, W. Shirley, N. Tantivasadakarn, and D. J. Williamson, PRX Quantum **3**, 010353 (2022).
[53] X. Chen, Z.-C. Gu, and X.-G. Wen, Phys. Rev. B **82**, 155138 (2010).
[54] S. Boyd and L. Vandenberghe, *Convex Optimization* (Cambridge University Press, Cambridge, England, 2004).
[55] J. Haah, Commun. Math. Phys. **324**, 351 (2013).
[56] Different fractional mobility structures impose distinct constraints on fracton statistics. The interplay will be interesting for future studies.